Heterogeneous Chemistry of HOBr on Different Types of Ice and on Ice Doped with HCl, HBr, and HNO_3 at 175 K < *T* < 215 K

L. Chaix,† A. Allanic,‡ and M. J. Rossi*

Laboratoire de Pollution Atmosphérique (LPA), Ecole Polytechnique Fédérale de Lausanne (EPFL), CH-1015 Lausanne, Switzerland

Received: March 16, 2000; In Final Form: May 25, 2000

The uptake kinetics of HOBr on ice with and without HX has been measured in a Teflon-coated low-pressure flow reactor (Knudsen cell) at temperatures of 175−205 K. The values of the initial uptake coefficient γ_0 of HOBr on different types of pure H_2O ice such as single-crystal ice, vapor-deposited ice, and samples frozen from liquid H_2O range from 0.4 to 0.03 and reveal a pronounced negative temperature dependence with an activation energy of $E_a = -9.7 \pm 1.0$ kcal/mol. The rate of HOBr uptake is independent of the type of ice. HOBr is able to sustain an equilibrium vapor pressure above an ice surface in the range from 185 to 210 K when sufficient HOBr has been adsorbed and is associated with an enthalpy change $\Delta H^0_r = -9.4 \pm 1.0$ kcal/mol. Adsorbed HNO_3 has no influence on the HOBr uptake coefficient on ice, even when the amount of HNO_3 contaminating the surface of ice is as high as 10 formal monolayers. The interaction of HOBr with HX-doped ice in the temperature range from 180 to 215 K leads to rapid formation of BrX at values of γ_0 of HOBr being less temperature dependent than for HOBr adsorption on pure ice: $E_a = -6.6 \pm 2.0$ kcal/mol has been found for the narrow temperature range from 195 to 215 K. The mass balance for BrCl from the reaction HOBr + HCl/ice is closed, in contrast to Br_2, which is the primary product of the reaction HOBr + HBr/ice. The uptake rate coefficients for HOBr + HCl/ice and HBr/ice are not significantly different from each other over the range from 180 to 215 K and are equal to $\gamma_0 = 0.3$ from 180 to 195 K, after which they drop with increasing temperature, but less so than for pure ice. At 205 K, γ_0 for HOBr + HX is typically a factor of 4 higher than γ_0 for HOBr uptake on pure ice. The atmospheric implications of these results are briefly discussed.

Introduction

It has recently been shown that both global and polar ozone depletion are intimately linked to heterogeneous processes occurring on background sulfuric acid aerosols or Polar Stratospheric Clouds.[1,2] Clear evidence of the importance of interfacial chemistry has been collected especially for Cl-containing species.[3] In addition, a significant impact of heterogeneous chemistry of Br-containing compounds on atmospheric chemistry is expected as a consequence of field observations which lead to a chemical mechanism that has subsequently found its way into models of ozone depletion.[4] As bromine is 100 times more efficient in terms of ozone destruction than chlorine on a mole-per-mole basis, it could play a significant role, on the order of 20%, in the formation of the ozone hole.[5,6] Bromine increases the rate of chlorine activation in the catalytic cycle of the lower stratosphere owing to the fast bimolecular reaction of ClO + BrO,[7] which is approximately a factor of 10^3 and 4×10^4 faster at 300 and 200 K, respectively, compared to the analogous ClO + ClO reaction.[8] The increasing importance of the mixed ClO/BrO reaction system with decreasing temperature is partly a consequence of its slight negative temperature dependence in contrast to the significant positive temperature dependence of the reaction ClO + ClO. Numerous aspects of the heterogeneous chemistry of bromine are still an active field of research.

The precursor to HOBr in the atmosphere is BrO as far as homogeneous gas-phase chemistry is concerned. Recently, the presence of BrO both in the stratosphere as well as in the troposphere has been confirmed using both remote sensing and *in situ* techniques that have established its spatial and temporal distribution. Using the sensitive technique of long pathlength differential optical absorption spectrometry (DOAS), Platt and co-workers were able to detect BrO locally in the planetary boundary layer in the proximity of the Dead Sea[9] at concentrations up to 86 ppt. This is in excess of the concentration measured in polar regions and a factor of approximately 6 above that measured in the stratosphere.[10,11] Sudden boundary layer ozone depletion events during the Arctic Spring have implied heterogeneous chemistry involving HOBr in what has been called the "Bromine Explosion" to indicate an autocatalytic branched chain in the presence of solar photons that rapidly activate inorganic bromine.[12] Even though the origin of the bromine is still uncertain, considerable efforts have been undertaken to quantify the temporal and spatial variation of BrO in the Arctic. McConnell and co-workers have detected large quantities of BrO above the Arctic during a summer campaign using remote sensing measurements on a high altitude research aircraft platform.[13] They came to the conclusion that most of the BrO occurred below 8 km, thus in the troposphere, even though the vertical distribution remained largely undetermined in their column density measurement. These observations together with satellite-mapping of tropospheric BrO[14,15] indicate that air masses enriched in BrO extend over large areas reaching maximum values of 20 to 60 ppt in proximity of sea ice.

* To whom correspondence should be addressed.
† Current Address: ST Microélectronique, Crolles (Grenoble), France.
‡ Current Address: Department of Chemistry, University College, Cork, Ireland.

10.1021/jp001018z CCC: $19.00
Published on Web 07/14/2000

Typically, these Arctic BrO concentrations are a factor of 5 to 10 above stratospheric background and are clearly correlated with events of boundary layer ozone losses occurring on the time scale of days.

Tropospheric bromine species mainly originate from both natural and synthetic sources. An important natural source of bromine is located in the oceans, which emit methyl bromide (CH_3Br) or bromoform ($CHBr_3$), the latter of which probably represents the most abundant reservoir of gas-phase bromine.[16] These natural sources cannot in general reach the stratosphere in view of their short tropospheric lifetimes. However, anthropogenic sources have sufficiently long tropospheric lifetimes such that they may represent a significant source of bromine in the stratosphere through occasional large-scale convective cloud-pumping events. These anthropogenic sources essentially are emissions caused by evaporation of agricultural fumigants or by biomass burning.[17] Halons used in fire-fighting equipment are also a major source of bromine transported to the stratosphere. It was recently concluded, on the basis of air samples archived in firn ice, that halons are exclusively of anthropogenic origin, whereas the concentration of CH_3Br has significantly increased in the 1970s and 1980s compared to the period between 1900 and 1970, probably as a result of its use as a fumigant.[18]

In the lower stratosphere and upper troposphere, the main bromine reservoir species are BrO, HOBr and $BrONO_2$,[19] and HBr.[20] The synergistic effect of BrO with ClO and the resulting efficiency in ozone destruction has been discussed above. In the stratosphere, $BrONO_2$ is generated by homogeneous recombination of BrO with NO_2 and is the most important reservoir species of bromine together with HOBr which is generated in the reaction of BrO with HO_2 in the gas phase:

$$BrO + HO_2 \rightarrow HOBr + O_2 \qquad \text{(R-1)}$$

During nighttime, $BrONO_2$ is destroyed by hydrolysis in heterogeneous processes on atmospheric particles containing H_2O according to:

$$BrONO_2 + H_2O \rightarrow HOBr + HNO_3 \qquad \text{(R-2)}$$

Reactions 1 and 2 are the most important generators of HOBr in the atmosphere. The observation of BrO in the stratosphere[21] proves that HOBr must play an important role in bromine chemistry related to catalytic ozone destruction, not only because it is a photolabile species,[22,23] but also because it is the primary product of the heterogeneous hydrolysis of $BrONO_2$ on ice (R-2). The presence of HOBr has also been invoked to explain the rapid onset of the OH and HO_2 concentration as well as their diurnal variation in the lower stratosphere.[24] To obtain a detailed understanding of the interaction of $BrONO_2$ with ice, it is necessary to examine the kinetic behavior of HOBr in the presence of various types of ice substrates that may be of atmospheric relevance. Chaix et al.[25] have recently shown that the kinetics of uptake of D_2O vapor can vary significantly from one type of ice substrate to another by as much as a factor of 4 in the temperature range from 140 to 210 K. We, therefore, ask the legitimate question, to what degree does the type of ice substrate control the interfacial kinetics of other relevant reactions that may occur on atmospheric ice particles. It is noteworthy that even in the absence of NO_x and therefore of $BrONO_2$ heterogeneous chemistry involving bromine may occur because HOBr may continue to be formed according to reaction 1.

Actually, only a few measurements of the HOBr uptake coefficient on ice substrates have been performed. The previous results have been obtained by Abbatt,[26] by Hanson and Ravishankara,[27] and more recently by Allanic et al.[28] and by Chu and Chu.[29] However, the results of Allanic et al.[28] seem to be in disagreement with the former two,[26,27] whereas they agree well with the latter.[29] In this paper, we present a more complete kinetics study of the interaction of HOBr with different types of ice as well as ice that has previously been exposed to known amounts of HCl, HBr, and HNO_3. Both pulsed valve time-resolved and steady-state experiments on the kinetics of adsorption of HOBr have been performed on well-characterized ice samples.

Experimental Section

All of the experiments have been performed using a Teflon coated Knudsen flow reactor that is part of a continuous flowing gas experiment. A detailed account of this technique has been given elsewhere.[30,31] Briefly, the reactor is mounted on a differentially pumped vacuum chamber fitted with a quadrupole mass spectrometer. After admission into the flow reactor the molecules effuse across the escape orifice of variable size. During their gas-phase lifetime (residence time) τ, which corresponds to the inverse of the measured effusion rate constant k_{esc}, the molecules interact with the surface of interest at a known collision frequency ω given by the geometric surface area of the sample. An effusing thermal molecular beam is formed at the escape orifice, which is monitored as a function of time using phase-sensitive mass spectrometric detection after it has been modulated using a rotating chopper wheel at a frequency of 150 Hz. The loss rate of the vapor phase over the ice is competing with the loss owing to diffusion through the escape aperture and is compared to reference experiments in which the interacting flow is isolated from the ice sample. Absolute concentrations of H_2O vapor are determined from a calibration of the MS signal at $m/e = 18$ with absolute flow rates of H_2O obtained by recording the H_2O pressure change in a calibrated volume as a function of time.

We have performed two types of experiments: continuous flow and pulsed valve experiments.[31] Most of the reported experiments have been performed in the continuous flow mode where flows of HOBr ranging from 10^{14} to 10^{16} molecule s^{-1} were introduced into the reactor. In reactive experiments, in which the ice sample is exposed to a measured HOBr flow, the source flow F^{i}_{HOBr} is balanced by two independent competing processes, namely the measured rate of escape F^{o}_{HOBr}, and the chemical interaction rate F_{het}, which is assumed to be first order in the HOBr concentration ([HOBr]):

$$F^{i}_{HOBr} = F^{o}_{HOBr} + F_{het} \text{ with } F_{het} = Vk_{eff}[HOBr] \qquad (1)$$

Because the effusion rate has been shown to be of first order, eq 1 directly leads to the expression for the rate constant k_{eff} for the heterogeneous interaction:

$$k_{eff} = ((S_o/S_i) - 1)k_{esc} \qquad (2)$$

where S_o and S_i are the MS signals of HOBr with the ice isolated and exposed to the HOBr flow, respectively. The values of k_{esc} could easily be determined from pulsed valve experiments as indicated in Table 1. For the 14 mm diameter aperture of the flow reactor, $k_{esc} = 3.0 \pm 0.3\ s^{-1}$ has been measured in good agreement with the calculated value $k_{esc} = 3.1\ s^{-1}$. We have not observed the expected deviation of the measured from the

TABLE 1: Characteristic Parameters of the Knudsen Flow Reactor[a]

definition	symbol	expression	numerical value[b]
reactor volume	V		1830 cm^3
sample surface area	A_s		17 cm^2
escape orifice diameter	D_0		14 mm
escape rate constant	k_{esc}	$1.77(T/M)^{0.5}$	3.1 s^{-1}
gas number density	N	$F^i_{HOBr}/(Vk_{esc})$	
collision frequency	ω	$34.7(T/M)^{0.5}$	61 s^{-1}

[a] F^i_{HOBr} is the continuous flow of HOBr into the Knudsen flow reactor. [b] Calculated at $T = 300$ K using $M = 97$amu as HOBr molar mass.

calculated value of k_{esc} for the 14 mm diameter orifice, however, the experimental value has a large uncertainty owing to the instability of HOBr in the flow reactor. Using this technique, we are able to follow the interaction of the gas phase with the reactive surface on a time scale extending up to several tens of minutes. We also have confirmed the results on the initial rate of uptake obtained in pulsed valve experiments when we compare it with the initial rate of uptake in continuous flow experiments just after lifting the isolation plunger. The uptake coefficient γ is determined from the measured rate constant k_{eff} according to eq 3 with the gas−surface collision frequency given by eq 4:

$$\gamma = k_{eff}/\omega \tag{3}$$

$$\omega = (\langle c \rangle/4V)A_s \tag{4}$$

where $\langle c \rangle$ is the average molecular velocity of the gas, A_s is the geometric surface of the ice sample exposed to HOBr, and V is the volume of the flow reactor (Table 1).

In view of the high values of the uptake coefficient for the HOBr-ice interaction, expression (4) is appropriate for evaluating the gas−surface collision frequency as it treats the total surface in terms of its geometrical projection onto a flat support plane: under this condition, a correction of γ using pore diffusion theory is unnecessary. HOBr never explores the depth of the ice substrate on our time scales ranging from a fraction to several seconds, instead it interacts only with the outer surface ("skin") of the sample. HOBr was monitored at $m/e = 98$, its molecular ion peak, which is an unambiguous marker for HOBr even in the presence of other bromine-containing gases such as $BrONO_2$ and Br_2O. Control experiments, in both continuous flow and pulsed valve mode clearly showed the absence of any interaction between HOBr and the internal walls of the Knudsen flow reactor.

Hypobromous acid, HOBr, is prepared from an aqueous solution according to the protocol described in reference:[32] 5 mL of liquid Br_2 is added drop by drop to 150 mL of distilled water at ambient temperature in which 24.5 g of $AgNO_3$ have previously been dissolved. This first step is completed after 30 min, after which the mixture was further agitated for another 10 min. The second step consists of a vacuum distillation where the condenser temperature is fixed at 273 K. The distillate is collected at 230 K in a trap containing 20 mL of 20% (wt) sulfuric acid meant to stabilize HOBr in solution. To improve the $HOBr/Br_2$ ratio the distillation was often conducted at a slow pace for 2 or 3 h. Br_2 extraction using CCl_4 was carried out as well in order to purify the final product. Yet, the frozen HOBr solution has to be melted and kept at 273 K prior to its use for the experiment. Therefore, the level of Br_2 contamination is significant, presumably because of thermal decomposition during synthesis and purification of HOBr. The thermal instability coupled to the high partial pressure of H_2O prompted us to look for an alternative HOBr source.

The second source is similar to the one used by Abbatt[26] and leads to the on-line generation of HOBr using an Evenson cavity connected to a microwave power supply operating at 2.45 GHz. OH free radicals were formed by passing a pure or dilute mixture of H_2O in He through the microwave cavity mounted upstream of the inlet to the Knudsen Cell. The inner wall of the inlet tube is coated with Teflon in order to avoid loss of OH on the walls. Pure Br_2 in excess was then added approximately 10 cm upstream of the reactor inlet but downstream of the H_2O discharge. Typical flow conditions were 10^{15} molecule s^{-1} H_2O and 10^{16} to 10^{17} molecule s^{-1} Br_2. HOBr was generated in the following reaction sequence:

$$H_2O \rightarrow OH + H \text{ (microwave discharge)} \tag{R-3}$$

$$OH + Br_2 \rightarrow HOBr + Br \tag{R-4}$$

The adjustment of each of the reactant flows allowed us to quantitatively titrate the OH free radicals by using excess Br_2. We ended up with a stable, "dry" source of HOBr containing a known amount of Br_2 and in which the degree of dissociation of H_2O to OH free radicals could be quantitatively monitored using the mass spectrometer ($m/e = 17$) in experiments of the type microwave power "on" and "off". The H_2O concentration in the final HOBr source could easily be monitored.

The HOBr flow was calibrated *in situ*. A cold support surface at 160 K was exposed to a measured flow of HOBr, a large and measured fraction of which condensed and was subsequently titrated by a known amount of HCl. At last the sample was allowed to heat up so as to evaporate the condensed phase. All through the procedure, BrCl was monitored during quantitative conversion of HOBr according to (R-5) for the whole length of the titration experiment. Having previously calibrated BrCl using an authentic sample, we were able to quantify the total amount of reacted HOBr by setting it equal to the observed amount of BrCl and thus calibrate the corresponding MS signal at $m/e = 96$ or 98.

$$HOBr + HCl \rightarrow BrCl + H_2O \tag{R-5}$$

The instability of HOBr led to some degree of decomposition already in the stagnant volume of the pulsed valve and therefore limited our ability to measure initial uptake coefficients γ_0 that were completely free of saturation. To obtain higher doses of HOBr longer valve opening times were chosen leading to competition between the two processes of interest, namely HOBr adsorption and desorption, and HOBr effusion already during the injection of HOBr into the Knudsen flow reactor.

To attain the temperature range of 140 to 220 K, we used a sample holder described elsewhere.[33] To test whether the sample preparation procedure had a significant impact on the uptake kinetics, three different types of ice samples have been prepared.[25] The first, referred to as bulk sample (B), consists of liquid degassed H_2O that has been poured into the dish of the sample holder at ambient temperature and rapidly frozen down to 160 K within approximately 4 min. This sample was subsequently annealed at 240 K during 20 min at a background pressure of several hundred Torr of N_2. To avoid the inclusion of air bubbles in the crystal, the liquid H_2O sample was previously degassed by freeze−pump−thaw cycles in a separate high vacuum line. The second, referred to as single-crystal ice (SC), has been obtained by freezing degassed deionized H_2O at a very slow rate on the order of 1/3 K/min in order to avoid the build-up of stress during crystal growth. We assume that this type of ice sample is characterized by very low surface

defect densities such as dislocations or cracks following literature reports. Another type of sample (C) has been obtained by condensation of water from the vapor phase by admitting a flow F^{i}_{H2O} into the Knudsen reactor and exposing it to the sample dish at the temperature of interest, namely 140 to 180 K. Exposure of this water flow to the cold copper substrate of the sample holder for a given time resulted in the deposition of a thick ice film equivalent to a few thousand monolayers depending on the amount of vapor condensed. The texture of the deposit may be porous, depending on the choice of the deposition temperature and F^{i}_{H2O}.[34] In addition, for ices condensed at 180 K the degree of crystallinity is known to depend on the deposition rate.[35] During the kinetic measurements, every ice sample has been kept at equilibrium under steady-state conditions by setting an additional constant external H_2O flow so as to balance evaporation, condensation and effusion rates on ice, thus resulting in no net H_2O uptake.

Results and Discussion

Pulsed-valve and steady-state experiments have been performed on different types of ice using both available sources of HOBr discussed above. To characterize the process of adsorption, we have investigated the dependence of the uptake kinetics on various parameters such as the temperature, the HOBr flow, the mode of formation of the ice samples, and the contamination of the surface by molecules of atmospheric interest that possess high affinity for ice (HCl, HBr and HNO_3).

HOBr on Ice. We have performed both pulsed valve and continuous flow experiments in which we have exposed a given amount of HOBr to a virgin ice sample. The injected pulse of HOBr ranged from 10^{15} to 10^{18} molecules per pulse, corresponding to a coverage on the ice sample from 10% to several formal monolayers, one monolayer corresponding to 5×10^{14} molecule cm^{-2} when we assume a HOBr cross section of 20 $Å^2$ according to known van der Waals radii. Steady-state experiments were conducted using the 14 mm escape aperture at flow rates F^{i}_{HOBr} leading to HOBr partial pressures in the range 10^{-6} to 5×10^{-4} Torr using relation (5) to calculate the partial pressure of HOBr:

$$P_{HOBr} = (F^{i}_{HOBr}/k_{esc}\, V)\, RT \qquad (5)$$

Figure 1 shows a typical pulsed valve (a) and steady state or continuous flow (b) experiment performed both at 200 K on a bulk ice sample. In both experiments, we clearly observed the formation of a steady-state level sometime after the start of the uptake as shown by the quantitative results discussed below. The interaction of HOBr with water−ice is strong, in contrast to HOCl, which has a very weak interaction with ice.[36] "Strong" and "weak" refer to the quantity of HOBr and HOCl, respectively, which are retained by the ice. As displayed in Figure 1(a), a quasi-steady-state level of the MS signal is maintained after the initial fast exponential drop once the bulk ice sample has been exposed to a pulse of 10^{15} HOBr molecules. The MS signal remains approximately constant for 0.3 s and finally decreases to its initial background level after a few seconds. The duration of the steady state level is proportional to the injected dose, whereas its amplitude is controlled by the balance between the rate of HOBr adsorption, evaporation and effusion, and only depends on temperature. The behavior of the transient signal is very similar to the one encountered for HCl/ice[37] and $D_2{}^{18}O/D_2{}^{16}O$ ice.[25]

Figure 1(b) displays a typical continuous-flow experiment where fresh bulk ice (B) at 200 K is exposed to a constant flow

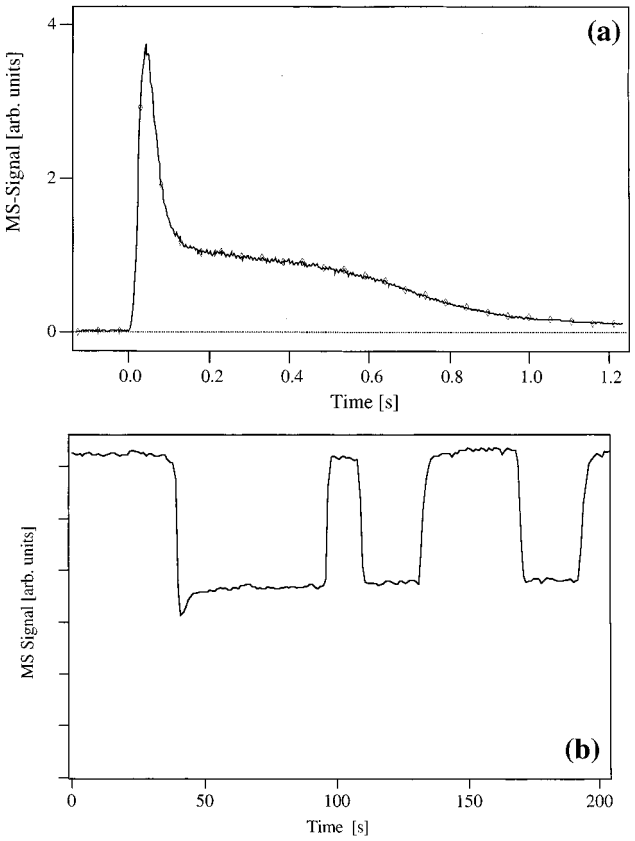

Figure 1. Typical pulsed valve (a) and continuous flow (b) experiments performed at 200 K on a bulk ice sample (B). For the pulsed valve experiment displayed in (a), the injected dose corresponds to a pulse of 10^{15} molecules. In (b) HOBr is let into the reactor at $F^{i}_{HOBr} = 6 \times 10^{14}$ molecule s^{-1} and monitored at 98 amu. The sample compartment is opened at $t = 40$ s and closed at $t = 95$ s. Two additional uptake experiments on the same ice sample have been subsequently recorded.

of HOBr at 6×10^{14} molecule s^{-1} monitored at *m/e* 98, corresponding to a partial pressure of 1.05×10^{11} molecule cm^{-3}. We first observed an initial high rate of uptake of HOBr leading to a low level MS signal ("spike") at $t = 40$ s, followed by a second higher steady-state level F^{ss} beginning at $t = 60$ s, which corresponds to a lower net uptake rate characterized by γ_{ss}. In the example displayed in Figure 1(b), the initial uptake rate constant and uptake coefficient were measured as $k_0 = 3.07$ s^{-1} and $\gamma_0 = 5 \times 10^{-2}$, respectively, whereas the corresponding values at steady state were $k_{ss} = 2.16$ s^{-1} and $\gamma_{ss} = 3.5 \times 10^{-2}$, respectively. The steady-state rate of uptake is interpreted as a partial saturation process, which points toward a complex uptake mechanism involving evaporation of HOBr under steady-state conditions that counteracts the HOBr adsorption on ice resulting in a net rate of uptake. The continued exposure of ice to HOBr in repetitive uptake experiments using the same ice substrate led to the same partial pressure of HOBr under steady-state conditions as shown in Figure 1(b) at times exceeding 60 s. Therefore, the high initial values γ_0 can only be obtained for the first HOBr exposure of a fresh ice sample.

In all cases, the interaction seems to be limited to physical adsorption of HOBr, as no reaction product, such as Br_2O, could be detected in the aftermath of the HOBr/ice interaction that is also in agreement with the results obtained by Chu and Chu.[29] Only in a few cases was a small rate of production of Br_2O, recorded at its molecular ion *m/e* 176, observed. It may be possible that in those cases, Br_2O may have been formed on some internal surface of the Knudsen cell and not on the surface

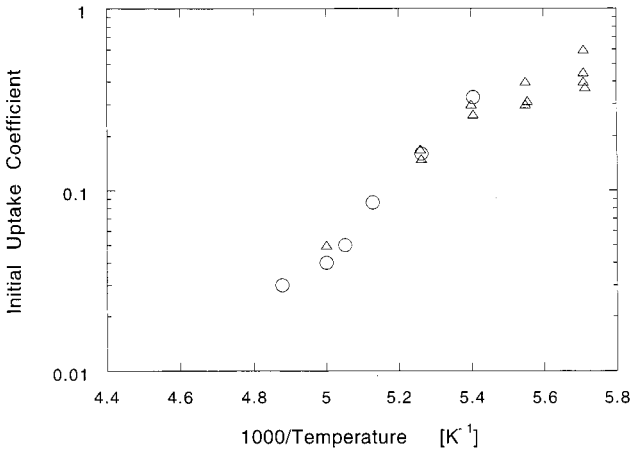

Figure 2. Initial uptake coefficient γ_0 of HOBr on a bulk ice sample (B) as a function of temperature for pulsed valve (triangles) and continuous flow experiments (circles) in the range 175 to 205 K.

of the ice sample. However, even if Br_2O was generated on the ice surface, the amount observed did not enable us to close the bromine mass balance. It is interesting to note in passing that in other instances Br_2O present as an impurity in the HOBr source, was observed to adsorb on the ice surface at low temperature ($T < 190$ K).

In this study, we interpreted the initial uptake leading to the low level MS Signal of HOBr as a kinetic process corresponding to the initial uptake coefficient γ_0 for the HOBr/ice heterogeneous interaction. In contrast to what has been observed for the interaction of HOCl on ice, HOBr obviously strongly interacts with the surface of ice. In the particular example of the experiment displayed in Figure 1(b), γ_0 at 200 K has been found to be roughly an order of magnitude larger than γ_0 obtained at the same temperature for HOCl ($\gamma_0 = 0.01$) where both experiments have been performed in the same Knudsen flow reactor.[36] In addition, the quantity of HOCl taken up corresponds to a fraction of a monolayer coverage on ice in contrast to the unlimited amounts of HOBr taken up on ice akin to HCl.[8]

In both types of experiments, continuous flow and pulsed, we have measured the initial uptake coefficients γ_0 of HOBr on ice as a function of the sample temperature. As is shown in Figure 2, all of the experiments performed on ice samples reveal a pronounced negative temperature dependence of γ_0. An Arrhenius plot of the initial uptake coefficient in the temperature range from 175 to 205 K results in a negative activation energy of 9.7 ± 1.0 kcal/mol. The values of γ_0 obtained in continuous-flow experiments on a fresh ice sample are in agreement with those obtained in pulsed-valve experiments within experimental uncertainty. We, therefore, conclude that both pulsed valve and steady-state experiments result in identical values of γ_0. In addition, there was no significant effect of the type of ice (B, C, or SC) on the value of γ_0 as displayed in Figure 3 and Table 2. This independence of γ_0 on the type of ice is in agreement with the fact that the interaction is strong, which therefore leads to the possibility that it significantly modifies the surface properties of the ice sample resulting from the interaction. This strong interaction will even out minor differences of the particular structural features of the substrates, as far as the uptake kinetics are concerned and is in stark contrast to the adsorption of $D_2{}^{18}O$ vapor on $D_2{}^{16}O$ ice where the interaction cannot lead to surface modification.[25] All experiments have been performed using both sources of HOBr. Figure 4 shows the initial uptake coefficient γ_0 obtained on bulk (B) ice using both sources, which

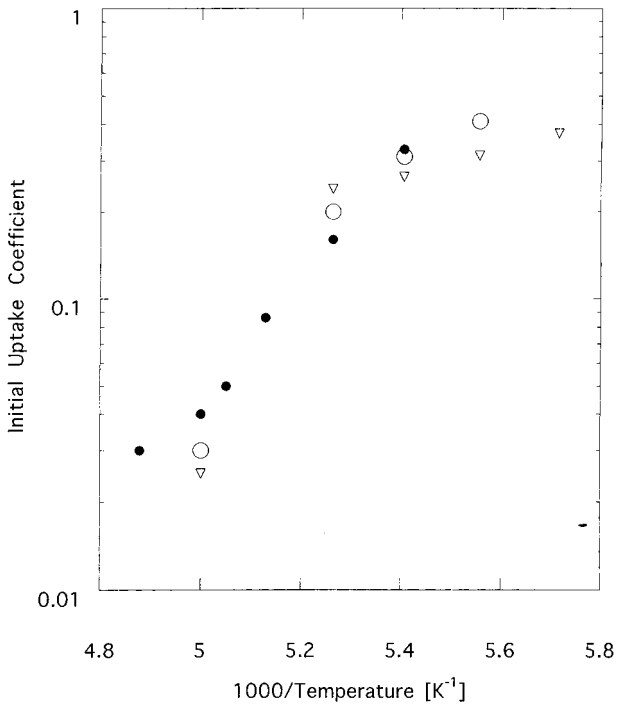

Figure 3. Initial uptake coefficient γ_0 of HOBr on single crystal (SC) (open circles), vapor-condensed (C) (open triangles) and bulk (B) ice (filled circles) measured in steady-state experiments in the temperature range 180 to 205 K.

TABLE 2: Initial and Steady-State Uptake Coefficients for HOBr Interacting with Pure Water Ice from Continuous Flow Experiments

T [K]	F^i_{HOBr} [mol s^{-1}]	γ_0	γ_{ss}	type of ice
185	1.5×10^{16}	0.33	0.2	B
190	3×10^{16}	0.16	0.09	B
200	4.5×10^{14}	0.05	0.039	B
200	1×10^{16}	0.041	0.03	B
210	2.1×10^{14}	0.019	0.015	B
210	1.5×10^{16}	0.02	0.014	B
180	1.8×10^{15}	0.41		SC
185	2×10^{15}	0.31		SC
190	3.5×10^{15}	0.2		SC
200	2×10^{15}	0.03		SC
175	4×10^{15}	0.37		C
180	4×10^{15}	0.31		C
185	2.5×10^{15}	0.26		C
190	3.1×10^{15}	0.24		C
200	5.8×10^{15}	0.07		C
180	3×10^{15}	0.4		B[a]
185	3.2×10^{15}	0.32		B
190	2.5×10^{15}	0.19		B[a]
195	9×10^{15}	0.086		B
198	4×10^{15}	0.05		B
200	3×10^{15}	0.04		B[a]
205	2.2×10^{15}	0.03		B
190	9.5×10^{14}	0.2		B doped with HNO3[a]
195	2.1×10^{15}	0.1		B doped with HNO3[a]
200	9×10^{14}	0.05		B doped with HNO3[a]

[a] Result obtained using the "dry" (microwave discharge) HOBr source.

leads to the conclusion that the kinetic results are independent of the type of source used. This also goes to show that the HOBr uptake is independent of the partial pressure of H_2O because γ_0 is the same both for the "dry" (microwave discharge) as well as the "wet" (batch) source.

These observations seemed to disagree at first with the measurements of γ_0 previously performed by Abbatt[26] because it appeared that his γ_0 values were significantly lower than the

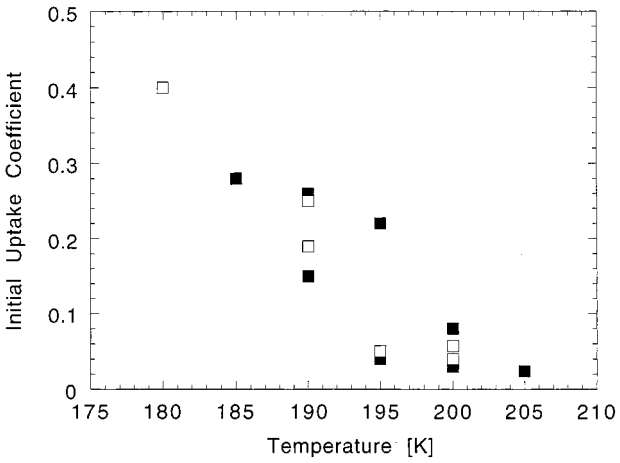

Figure 4. Initial uptake coefficient γ_0 measured in steady-state experiments of HOBr interacting with bulk (B) ice as a function of temperature. HOBr has been prepared using the batch mode (filled squares) and microwave discharge-based *in situ* generation (open squares).

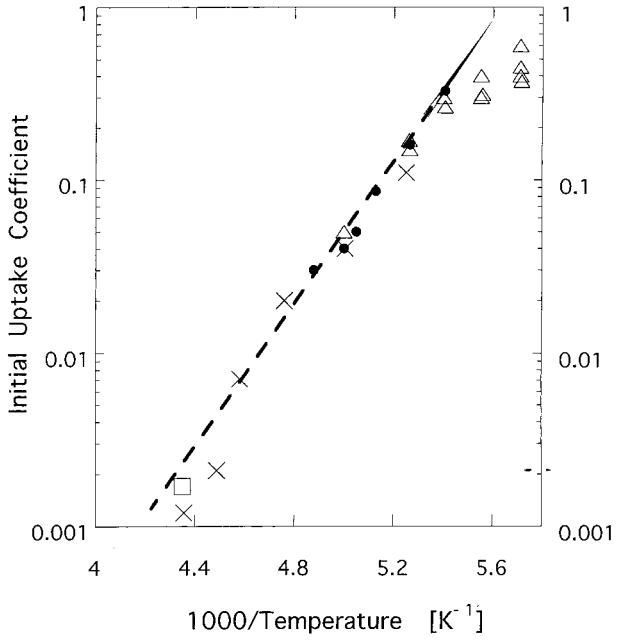

Figure 5. Comparison of the initial uptake coefficient γ_0 of HOBr on water ice as a function of temperature: Abbatt[26] (open square at 228 K, vapor-condensed (C) ice), Chu and Chu[29] (*x*, vapor-condensed (C) ice) and present work (pulsed valve experiment: open triangles, continuous flow experiment: filled circles, both series on bulk (B) ice). The straight dashed line corresponds to an activation energy of $E_a = -9.7 \pm 1.0$ kcal/mol.

ones obtained in this work. In fact, Abbatt has performed his measurements at higher temperature (228 K) for which the values of γ are low, on the order of 2.0×10^{-3}. However, if one takes into account the pronounced negative temperature dependence of γ_0 resulting from this work, one notes the excellent agreement between the data of Abbatt,[26] Chu and Chu[29] and the present work shown in Figure 5. However, we must point out the unusual magnitude of the negative activation energy for an adsorption process whose mechanism together with chemical kinetic modeling will be discussed in a forthcoming publication.[38]

Additional experiments have been performed with the goal to investigate the flow rate dependence of γ_0 in order to determine the rate law of HOBr adsorption on ice. Results have

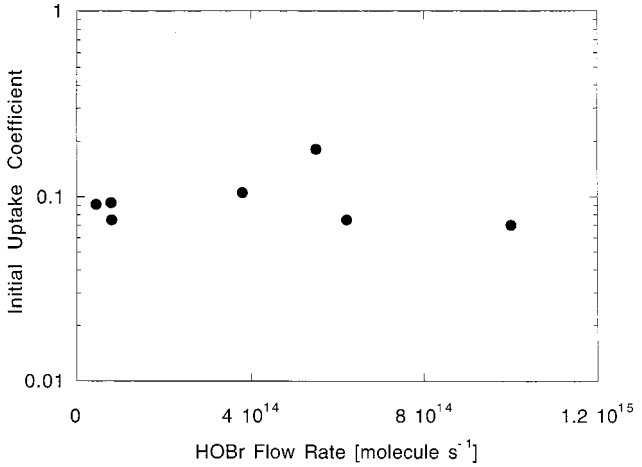

Figure 6. Flow rate dependence of the initial uptake coefficient γ_0 of HOBr adsorption on bulk ice (B) at 200 K from steady-state measurements.

been obtained at 200 K for a condensed ice sample (C) in steady-state experiments, and are displayed in Figure 6 where the measured flow rate of HOBr has been varied over 2 orders of magnitude. The lower limit is given by the sensitivity of the mass spectrometer for HOBr, the upper limit was imposed by the Knudsen conditions for maintaining the molecular flow regime. No concentration dependence of γ_0 has been observed at this temperature. All of the results presented above reveal an apparent first-order rate law for the uptake of HOBr on ice although the pronounced negative temperature dependence of γ_0 displayed in Figure 5 points toward the existence of an intermediate.

At sufficiently large injected doses or flows of HOBr, we have consistently observed a partial saturation of the initial uptake coefficient γ_0 leading to a steady-state level with a lower rate of uptake given by γ_{ss}, such as displayed in Figure 1(b) at $t = 60$ s. The formation of this steady state rate of uptake shows that an ice surface that has been exposed to HOBr is able to sustain a vapor pressure of HOBr, even after the source is shut off, as long as there is a sufficient quantity of adsorbed HOBr on the ice substrate able to support a vapor pressure for a sufficiently long time so it can be measured. The partial pressure of HOBr at equilibrium, P_{HOBr}, is calculated using results from either transient pulsed-valve or continuous flow experiments. P_{HOBr} may be calculated using eq 6, which uses data from individual pulsed valve or continuous flow experiments:[37]

$$P_{HOBr} = F^{ss}(1 + k_{eff}/k_{esc})\,(RT/k_{eff}\,V) \qquad (6)$$

where F^{ss} is the measured steady-state flow rate of HOBr under steady-state conditions or in the aftermath of a pulse (see Figure 1(a) or 1(b)), and k_{eff} is the corresponding measured rate constant for adsorption of HOBr on a fresh ice substrate (see Table 1 for the definition of the remaining symbols). We have used the experimental HOBr MS signals obtained under steady-state conditions and have calculated P_{HOBr} according to eq 6, which strongly depends on the initial pressure of HOBr defined as $P^i_{HOBr} = F^i_{HOBr}/Vk_{esc}$ as shown in Figure 7. P^i_{HOBr} is the partial pressure of HOBr at the given flow F^i_{HOBr} of HOBr into the flow reactor in the absence of an ice sample. A constant equilibrium vapor pressure P_{HOBr} corresponding to a limiting high value of F^{ss}, is obtained at sufficiently high values of P^i_{HOBr} and thus of F^i_{HOBr} as shown in Figure 7. At P^i_{HOBr} in excess of 10^{-4} Torr the values of P_{HOBr} become independent of P^i_{HOBr}.

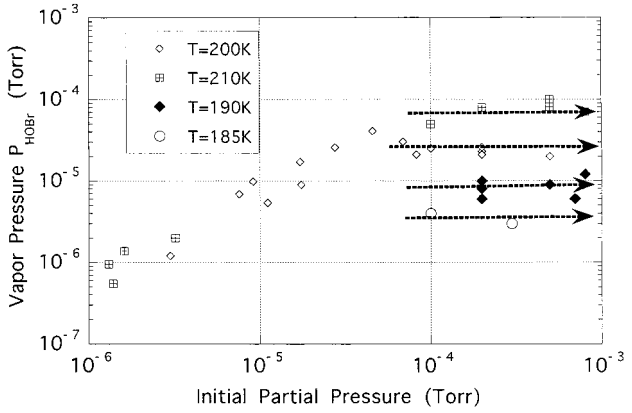

Figure 7. Calculated equilibrium partial pressure of HOBr, P_{HOBr}, in the temperature range 185−210 K above bulk ice (B). The equilibrium vapor pressure is the limiting value represented by horizontal arrows obtained beyond a sufficiently high initial partial pressure of HOBr into the reactor defined as $P^{i}_{HOBr} = F^{i}_{HOBr}/(k_{esc}\ V) > 10^{-4}$ Torr.

At that point, P_{HOBr} may be regarded as the equilibrium vapor pressure of HOBr over ice corresponding to evaporation of HOBr from an aqueous solution located at the interface between the gas phase and the ice.

The establishment of a partial pressure of HOBr over ice is very similar to what has been observed for the HCl/ice substrate where the same phenomenon has been observed in both steady state and pulsed valve experiments.[37] The results have been interpreted in terms of a mechanism involving the adsorption and subsequent ionization of HCl at the interface, HCl desorption, and a partial loss of HCl into the bulk by diffusion, which may also be valid for the case of the HOBr/ice system. As expected, the HOBr equilibrium vapor pressure over ice is strongly affected by temperature as shown in Figure 7. The temperature dependence of P_{HOBr} over ice as well as its independence on P^{i}_{HOBr} beyond a threshold pressure whose upper limit seems to be 10^{-4} Torr (Figure 7) leads us to the interpretation that a liquid HOBr/H_2O mixture atop the surface of the ice sample is supporting the equilibrium vapor pressure P_{HOBr}.

In this case, HOBr may either be electrolytically dissociated in the liquid film located on top of the ice sample depending on pH akin to the interaction in the HCl/ice system[37] or it may form stable hydrates, or both. This latter possibility is preferred in cases where HOBr interacts with ice that is contaminated with traces of a strong acid such as HNO_3 or H_2SO_4 because the low pH prevents HOBr from dissociating in view of its high p*K* value. The present experiments are unable to provide proof for either assumption on the final state of adsorbed HOBr, but they present compelling evidence of a kinetic intermediate in the precursor-mediated adsorption of HOBr on ice. A detailed chemical-kinetic mechanism of the interaction of H_2O, HCl, and HOBr with ice will be published elsewhere.[38]

A Van't Hoff plot in the range from 185 to 210 K of P_{HOBr} whose values are displayed in Figure 7 for $P^{i}_{HOBr} > 10^{-4}$ Torr leads to an enthalpy change $\Delta H^{0}_{r} = -9.4 \pm 1.0$ kcal/mol. We interpret this ΔH^{0}_{r} value as the enthalpy of evaporation of HOBr dissolved in an aqueous layer located on top of the ice interface region. As a consistency check, we have established the temperature dependence of the individual rate processes describing the adsorption/desorption of HOBr on ice, namely

$$\mathrm{HOBr\ (g) + H_2O\ (B) \underset{R_{des}}{\overset{k_{ads}}{\rightleftharpoons}} H^+ + BrO^-,}$$

$$\mathrm{HOBr.nH_2O\ or\ H_3O^+BrO^-.nH_2O} \quad \text{(R-6)}$$

using the Arrhenius representation of both the adsorption rate constant k_{ads} ($= k_{eff}$) and the rate of desorption R_{des} over the narrow temperature range 185−210 K. The evaporation rate of HOBr is given by eq 7:

$$R_{des} = (P_{HOBr}\, k_{eff}/RT) \text{ with } T = 300\ \mathrm{K} \qquad (7)$$

The result is $E_a(\mathrm{des}) = 0.8 \pm 0.2$ kcal/mol and $E_a(\mathrm{ads}) = -9.7 \pm 1.0$ kcal/mol resulting in $\Delta H^{0}_{r} = E_a(\mathrm{ads}) - E_a(\mathrm{des}) = -10.5 \pm 1.0$ kcal/mol, which is identical to the enthalpy change obtained from the Van't Hoff plot of the equilibrium vapor pressure P_{HOBr} within the experimental uncertainty. The existence of a HOBr vapor pressure over ice modifies the reaction mechanism proposed by Chu and Chu[29] in the sense that the interaction now becomes fully reversible. Once again it has to be pointed out that essentially the whole exothermicity of the interaction of HOBr with ice is contained in the adsorption process instead of the desorption rate as is usually the case. The interpretation revolves around an intermediate whose rearrangement into the final (bulk) state is entropically controlled.[38]

Upon heating the substrate following its exposure to a flow of HOBr, the steady state vapor pressure is observed to increase up to the point at which the supply of condensed phase HOBr starts to vanish. During these experiments, a significant fraction of the HOBr taken up on the ice could be recovered in the gas phase when the source of HOBr was only marginally contaminated by Br_2. The mass balance could thus be closed because no product accounting for the missing HOBr had been observed. The closed mass balance, the existence of an equilibrium vapor pressure, and the independence of γ_0 on the type of ice sample all point to the existence of a saturated layer atop the ice or a liquid overlayer. It is important to note that under identical experimental conditions, HOCl does not significantly interact with ice nor does it support a vapor pressure over ice,[36] whereas the strong interaction of HOBr with ice may enhance the efficiency of bimolecular heterogeneous reactions such as HOBr + HCl and HOBr + HBr under atmospheric conditions by following a Langmuir−Hinshelwood rather than an Eley−Rideal mechanism. In the case of HOBr, the heterogeneous reaction with HX may in fact occur exclusively in the condensed phase as a bimolecular reaction between two solvated species.

HOBr on HNO3-Doped Ice. Together with HNO_3, HOBr is the primary product resulting from the heterogeneous reaction (R-2) of $BrONO_2$ on ice:

$$\mathrm{BrONO_2 + H_2O \rightarrow HNO_3 + HOBr} \qquad \text{(R-2)}$$

During this reaction, HNO_3 is continuously formed and retained on the surface of the ice. For this reason, and in order to describe the primary process of $BrONO_2$ interaction with ice, it is important to study the kinetic behavior of HOBr on HNO_3 doped ice. To examine the influence of HNO_3 on the uptake of HOBr on ice substrates, we have performed HOBr uptake experiments on HNO_3-doped ice samples. The levels of doping correspond to an amount of HNO_3 between 0.1 and 3 formal monolayers, where 6×10^{14} molecules cm^{-2} form one monolayer. Pulsed-valve and continuous flow experiments have been performed on ice using both available HOBr sources as presented above, which resulted in identical values of the uptake coefficient within experimental uncertainty. The results are displayed in Figure 8, which shows that the γ values for the interaction of HOBr on HNO_3-doped ice seem to be larger in comparison with the ones obtained on pure ice. However, we conclude that there is no significant influence of adsorbed HNO_3

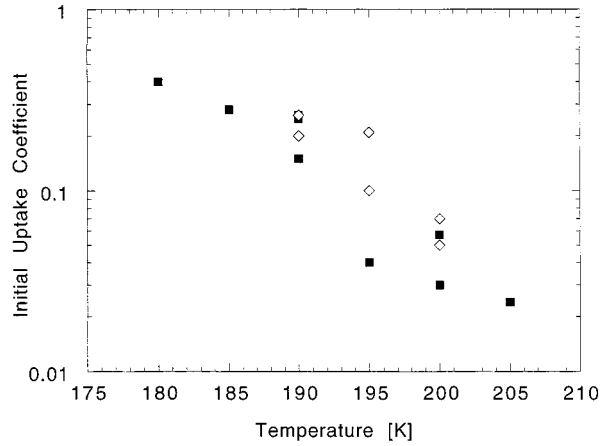

Figure 8. Initial uptake coefficient γ_0 of HOBr measured on bulk (B) ice (filled squares) and on a HNO_3-doped ice sample (open diamonds) as a function of temperature.

on the HOBr uptake coefficient within the limits stated above and that the values are therefore identical to the ones obtained for pure ice substrates. In addition, P_{HOBr} was independent of the HNO_3 doping levels within the stated limits, which means that dissolved HOBr and HNO_3 both support a vapor pressure independent of each other's presence within the concentration limits and temperatures used of this study.

HOBr On Ice/HCl and Ice/HBr. In the presence of HX (HCl, HBr) adsorbed on the ice surface, HOBr may undergo two different competing reactions leading to its disappearance from the gas phase: first, the mere condensation on the ice surface discussed above, and second, the halogen exchange reaction (R-7):

$$HOBr + HX \rightarrow BrX + H_2O \qquad (R\text{-}7)$$

Both pulsed-valve and continuous flow experiments were performed on different types of HX-doped ice samples, using both sources of HOBr. We adopted two standard protocols to dope the ice samples using an external flow of HX, namely a consecutive and a simultaneous flow technique. The consecutive method proceeded in two steps: the ice surface was first exposed to a known external flow of HX in order to enable the determination of the total dose deposited on the ice substrate. Then, once the HX flow had been halted, the HOBr was subsequently introduced into the reactor. Typical flow rates of HX used to dope the surface of ice ranged from 10^{14} to 10^{16} molecule s^{-1} leading to the deposition of 0.5 to 10 formal monolayers of HX onto ice depending on the deposition time.

In the simultaneous exposure technique, measured flows of HOBr and HX were admitted into the reactor and allowed to interact with the ice substrate in each other's presence. The experimental results showed that no significant difference in the kinetics was observed between the two experimental protocols. In both cases, HOBr was readily taken up by the doped ice surface, which was kept at equilibrium by setting additional, external H_2O and HX flows to prevent any net evaporation of H_2O or HX thereby resulting in a constant composition of the interface as far as both H_2O and HX are concerned. Because neither BrCl nor Br_2 significantly interact with water ice in the temperature range of interest, poisoning of the ice surface was not expected to occur when reacting HOBr with HCl. Large amounts of adsorbed HBr, however, may well form stable trihalide complexes at the ice interface.[39]

Various levels of HX-doping were used with flows ranging from 10^{14} (low) to 10^{16} (high) molecule s^{-1} in order to assess the role of the condensed phase HX in its reaction with HOBr. Flückiger et al. have shown that two different levels of HCl doping correspond to different domains in the ice/HCl phase diagram, namely the quasi-liquid and the solution (liquid) region at low and high HCl flow rates, respectively.[37] Subsequently, two typical doping levels of HX were consistently used: one corresponding to a doping level of less than a monolayer leading to a quasi-liquid state for HCl, and the other leading to the adsorption of a large amount of HX (up to 10 monolayers) forming an aqueous solution of HCl on top of the ice substrate.

In the case of both HCl and HBr, the interaction between HOBr and the HX-doped ice substrate leads to rapid formation of BrX. Its release in the gas phase is immediate and its rate of formation remains constant until the amount of HX available on the surface is essentially consumed, which may be the case for consecutive flow experiments. The HOBr signal then gradually increases toward a steady state value similarly to what was observed on pure ice surfaces indicating a slower rate of uptake. Eventually, once all the HX has reacted the HOBr partial pressure P_{HOBr} reaches the equilibrium vapor pressure measured at steady-state conditions over pure ice at the same temperature.

In the early stage of its exposure to HX-doped ice, HOBr mainly reacts with HX. At low HX-doping level or if the supply of HX after prolonged reaction starts to wane, the nonreactive adsorption of HOBr on the ice sample becomes dominant. This occurs independently of the type of ice used and indicates that most of the adsorbed HX is concentrated in the interface region in agreement with the fact that the HCl diffusion rate into bulk ice takes place on a longer time scale.[37]

In the frame of simultaneous-flow experiments, discrepancies were observed in the behavior of the HOBr signal depending on whether the ice was doped with HCl or with HBr. The HCl-doped ice sustains a vapor pressure of HOBr even after the HOBr source has been shut off, which is not the case for the HBr-doped ice, for which the signal of HOBr instantly reverts to zero once the HOBr source is shut off.

We interpret this observation in the sense that in the case of HBr-doped ice the adsorbed HOBr instantly reacts with adsorbed HBr in the condensed phase such that no reservoir of condensed phase HOBr would immediately be available to establish a vapor pressure once the HBr source has been turned off. In contrast, the condensed phase reaction of HOBr and HCl is slow enough to allow for the accumulation of condensed phase HOBr in sufficient quantities able to maintain a vapor pressure once the flow of HOBr is turned off. In both cases, the HOBr signal gradually increases to a steady state value similar to the one observed on pure ice surfaces under conditions of waning HX supply at the interface.

However, both types of experiments, that is sequential and consecutive exposure of HOBr, resulted in the same kinetic results on the rate of uptake of HOBr. The uptake coefficients are summarized in Table 3, Figures 9 and 10. By simultaneously measuring the rate of formation of BrCl and the disappearance of HOBr, we are able to close the mass balance for HOBr interacting with HCl-doped ice at excess HCl. As long as the reaction with HCl remains dominant and follows reaction (R-7), the number of molecules of HOBr lost on the ice surface is equivalent to the number of BrCl molecules produced. If the HOBr uptake experiment continues after HCl has been totally consumed the disappearance of HOBr is not accompanied by the appearance of a product any more.

For the reaction of HOBr with HBr, the mass balance could not be closed. This may have two reasons: (a) HBr may form stable hydrates on ice that are kinetically stable with respect to

TABLE 3: Initial Uptake Coefficients for the Reaction HOBr + HX (X = Cl, Br) on Water Ice at Various Temperatures

T [K]	γ_0	type of ice
195	0.38	B-type ice with simultaneous flow of HCl
200	0.15	B-type ice with simultaneous flow of HCl
205	0.08	B-type ice with simultaneous flow of HCl
210	0.11	B-type ice with simultaneous flow of HCl
215	0.08	B-type ice with simultaneous flow of HCl
180	0.44	B-type ice with simultaneous flow of HBr
185	0.39	B-type ice with simultaneous flow of HBr
190	0.36	B-type ice with simultaneous flow of HBr
195	0.33	B-type ice with simultaneous flow of HBr
200	0.23	B-type ice with simultaneous flow of HBr
205	0.17	B-type ice with simultaneous flow of HBr
180	0.4	C-type ice doped with HCl
190	0.35	C-type ice doped with HCl
200	0.11	C-type ice doped with HCl
210	0.14	C-type ice doped with HCl
185	0.4	C-type ice doped with HBr
190	0.38	C-type ice doped with HBr
195	0.28	C-type ice doped with HBr
200	0.18	C-type ice doped with HBr
205	0.15	C-type ice doped with HBr

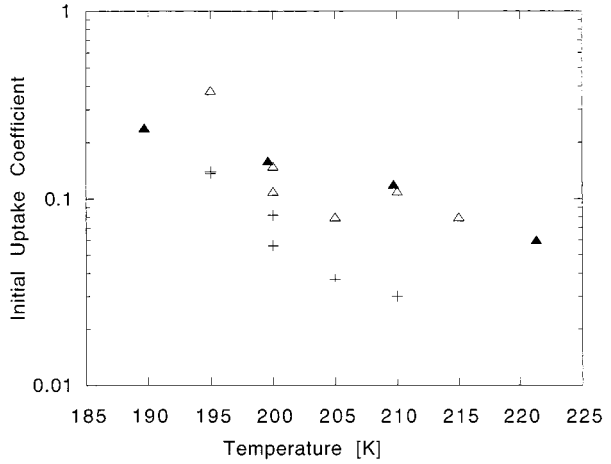

Figure 9. Initial uptake coefficient γ_0 of HOBr measured on bulk (B) ice (crosses) and HCl-doped ice (both simultaneous and sequential exposure, open triangles) as a function of temperature in comparison with results of Chu and Chu[29] (vapor-condensed (C) ice, filled triangles).

reaction with HOBr,[40] or (b) the reaction product Br_2 resulting from reaction (R-7) forms a stable trihalide complex with HBr of the type $H_3O^+Br_3^-$, thus preventing the detection of Br_2.[39] Other reactions where the bromine mass balance could not be closed as well include the reactions of N_2O_5 + HBr and HONO + HBr on ice in the temperature range from 180 to 210 K.[41,42]

As shown in Figure 10, the doping conditions (consecutive or simultaneous) do not significantly affect the initial uptake coefficients γ_0 of HOBr in the presence of both HCl and HBr. These values are consistently higher than the ones obtained on pure ice under similar conditions at $T > 195$ K. The γ_0 values are indistinguishable from the pure ice case for $T < 195$ K and are independent of the type of ice used for the experiment over the whole temperature range from 180 to 215 K. As was the case for pure ice the initial uptake coefficient γ_0 for the bimolecular reaction HOBr + HX is also independent of the flow rate of HOBr, that is the partial pressure of HOBr, and therefore follows an apparent first-order rate law. A negative temperature dependence of γ_0 for both reactions is observed with an activation energy $E_a = -6.6 \pm 2.0$ kcal/mol that is less pronounced than for the uptake of HOBr on water ice. Thus,

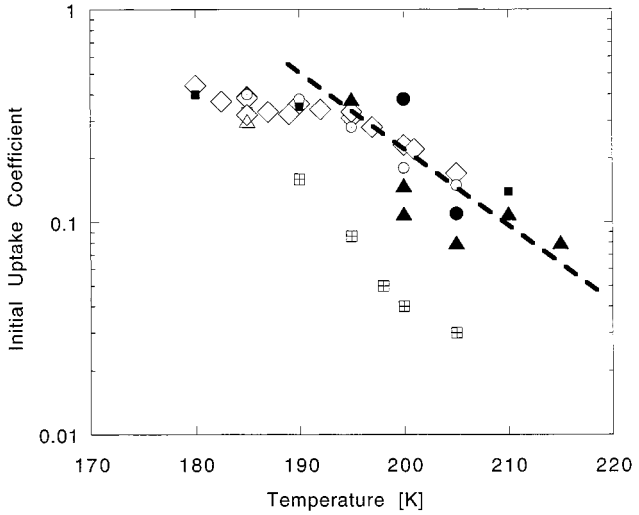

Figure 10. Summary of the measurements of the initial uptake coefficient γ_0 of HOBr measured in continuous flow experiments as a function of temperature: bulk (B) ice (open triangle, crossed squares); B-type ice with concurrent flow of HCl (full circles, full triangles); consecutive flow method: C-type ice doped with HCl (full squares); B-type ice with concurrent flow of HBr (open diamonds); C-type ice with concurrent flow of HBr (open circle). The straight line corresponds to an activation energy of $E_a = -6.6 \pm 2.0$ kcal/mol in the temperature range from 195 to 215 K.

as was the case for HOCl,[36] the presence of HCl on the fresh ice sample enhances the rate of uptake of HOBr by approximately a factor of 10 at 205 K in agreement with the results obtained by Chu and Chu.[29]

Atmospheric Significance. The importance of HOBr in heterogeneous chemistry is significant, because the hydrolysis of $BrONO_2$ allows HOBr to become the most important form of nighttime bromine in the stratosphere. In addition, HOBr is a major bromine reservoir in cases of low NO_x concentrations in the atmosphere and is capable of carrying on chlorine activation through heterogeneous reactions. Thus, the strong interaction of HOBr with the ice interface could lead to an increase in the concentration of halogenated radical species such as Br, Cl, and BrO in the absence of NO_x as a result of the heterogeneous reaction of adsorbed HX on the surface leading to BrX and ultimately to atomic halogens. The interaction of HOBr on ice particles enhances the conversion of a stable reservoir of chlorine and bromine (HCl and HBr) into a photolabile active form such as BrCl and Br_2. The result of this study shows that the reaction of HOBr with HX increases the conversion of HX into an active form of molecular halogen under all conditions attained in this study.

Conclusion

Pulsed valve and continuous flow experiments have been used to measure the interaction of HOBr on different types of ice samples (B-, C-, and SC-type), at temperatures in the range 170−220 K. In all cases, γ_0 values obtained in steady-state experiments are in agreement with those obtained in pulsed valve experiments within experimental uncertainty. The initial uptake coefficient γ_0 was observed to decrease with temperature and varied between 0.4 and 0.03 independently of the type of ice sample and of HOBr source (batch or *in situ* microwave-powered). This decrease of γ_0 with increasing ice temperature is consistent with the establishment of an equilibrium vapor pressure of HOBr above ice, which is constant beyond a threshold partial pressure. The decrease of γ_0 toward lower steady-state values γ_{ss} results from the evaporation of HOBr,

which counteracts the adsorption and therefore apparently leads to partial saturation of the HOBr uptake. This interaction is a nonreactive adsorption as no reaction product has been detected. The strong negative temperature dependence of γ_0 with $E_a = -9.7 \pm 1.0$ kcal/mol reconciles our kinetic results with those of Abbatt[26] and agrees with the results of Chu and Chu.[29]

The HOBr gas-phase density has been varied by an order of magnitude without observing a flow rate dependence of γ_0. This result reveals an apparent first-order rate law for the uptake of HOBr on ice despite its pronounced negative temperature dependence. All of these facts point towards a complex reaction mechanism implying that the interaction of HOBr with ice is not an elementary reaction. The partial saturation of γ_0 and the establishment of a vapor pressure above ice are systematically observed and depend on temperature only. This behavior is very similar to the interaction of HCl with ice.[37] Similarly, we propose the following mechanism of HOBr uptake on ice:

$$\mathrm{HOBr\ (g) + H_2O\ (B) \rightleftarrows HOBr_{(ads)} \rightleftarrows}$$
$$\mathrm{H^+ + BrO^-,\ HOBr.nH_2O\ or\ H_3O^+BrO^-.nH_2O} \quad \text{(R-8)}$$

which leads either to electrolytic dissociation or stable hydrate formation, or both. The partial saturation of γ_0 to γ_{ss} with the build-up of a vapor pressure P_{HOBr} as well as the strong negative temperature dependence of γ_0, and thus the existence of a precursor to HOBr adsorption, are all consistent with (R-8). The negative temperature dependence of P_{HOBr} reveals the enthalpy of evaporation of HOBr that has been measured as $\Delta H^0_r = -9.4 \pm 1.0$ kcal/mol.

The HOBr concentration used in this study was approximately 2 to 3 orders of magnitude higher than the actual HOBr concentrations thought to prevail in the stratosphere. However, the measurements of γ_0 were performed using HOBr doses amounting to a fraction of a monolayer in pulsed-valve experiments. We do not expect any mechanistic change in the HOBr adsorption in the submonolayer range and assert that our results can reasonably be extrapolated to stratospheric conditions, namely at much more dilute HOBr partial pressures.

Our results do not show any significant influence of HNO_3 adsorbed on ice on γ_0 and γ_{ss}. This result may be important under atmospheric conditions because HNO_3 is the primary product resulting from many heterogeneous reactions, which could modify the surface properties of ice particles. In the presence of HCl or HBr on ice, there is competition between HOBr nonreactive adsorption (R-8) and reaction (R-7). The interaction between HOBr and HX-doped ice leads to rapid formation of BrX, with a value of γ_0 that is less temperature dependent and generally larger than γ_0 observed on pure ice. The production of BrX allows one to close the mass balance in the case of HCl. A mass balance has not been established for reaction of HOBr on HBr-doped ice, in part because of mechanistic complications such as the formation of a stable trihalide on the ice substrate thus preventing the observation of Br_2 and in part because of large amounts of Br_2 in the HOBr source.

Acknowledgment. Funding for this work was generously provided by the Office Fédéral de l'Enseignement et de la Science (OFES) in the framework of the subproject COBRA of the EU program "Environment and Climate". We thank professor H. van den Bergh for his enduring support as well as his lively interest.

References and Notes

(1) Solomon, S.; Garcia, R. R.; Rowland, F. S.; Wuebbles, D. J. *Nature* **1986**, *321*, 755.
(2) Scientific Assessment of Ozone Depletion: 1998, World Meteorological Organization Global Ozone Research and Monitoring Project, Report No. 44, Global Ozone Observing System (GO_3OS).
(3) Molina, M. J. In *The Chemistry of the Atmosphere: its Impact on Global Change*; Calvert, B. J., Ed.; Oxford: United Kingdom, 1994.
(4) Barrie, L. A.; Bottenheim, J. W.; Schnell, R. C.; Crutzen, P. J.; Rasmussen, R. A. *Nature* **1994**, *334*, 665.
(5) McElroy, M. B.; Salawitch, R. J.; Wofsy, S. C.; Logan J. A. *Nature*, **1986**, *321*, 759.
(6) McConnell, J. C.; Henderson, G. S. *The Tropospheric Chemistry of Ozone in the Polar Regions*; Niki, H., Becker, K. H., Eds.; NATO ASI, 1993, *17*, 89.
(7) LeBras, G.; Platt, U. *Geophys. Res. Lett.* **1995**, *22*, 599.
(8) Atkinson, R.; Baulch, D. L.; Cox, R. A.; Hampson, R. F., Jr.; Kerr, J. A.; Rossi, M. J.; Troe, J. *J. Phys. Chem. Ref. Data* **1997**, *26*, 521.
(9) Hebestreit, K.; Stutz, J.; Rosen, D.; Matveiv, V.; Peleg, M.; Luria, M.; Platt, U. *Science* **1999**, *283*, 55.
(10) Arpag, K. H.; Johnston, P. V.; Miller, H. L.; Sanders, R. W.; Solomon, S. *J. Geophys. Res.* **1994**, *99*, 8175.
(11) Ferlemann, F. et al. *Geophys. Res. Lett.* **1998**, *25*, 3847.
(12) Barrie, L.; Platt, U. *Tellus* **1997**, *49B*, 450.
(13) McElroy, C. T.; McLinden, C. A.; McConnell, J. C. *Nature* **1999**, *397*, 338.
(14) Wagner, T.; Platt, U. *Nature* **1998**, *395*, 486.
(15) Richter, A.; Wittrock, F.; Eisinger, M.; Burrows, J. P. *Geophys. Res. Lett.* **1998**, *25*, 2683.
(16) Lary, D. J. *J. Geophys. Res.* **1996**, *101*, 1505.
(17) Khalil, M. A.; Rasmussen, R. A.; Gunawerdena, R. *J. Geophys. Res.* **1993**, *98*, 2896.
(18) Butler, J. H. et al. *Nature* **1999**, *399*, 749.
(19) Wayne, R. P. *Eur. Comm.* **1995**, Brussels.
(20) Nolt, G. et al. *Geophys. Res. Lett.* **1997**, *24*, 281.
(21) Orlando, J.; Burkholder, J. *J. Phys. Chem.* **1995**, *99*, 1143.
(22) Lary, D. J.; Chipperfield, M. P.; Toumi, R.; Lenton, T. *J. Geophys. Res.* **1996**, *101(D1)*, 1489.
(23) Ingham, T.; Bauer, D.; Landgraf, J.; Crowley, J. N.; *J. Phys. Chem.* **1998**, *102*, 3293.
(24) Wennberg, P. O. et al. *Science* **1994**, *266*, 398.
(25) Chaix, L.; van den Bergh, H.; Rossi, M. J. *J. Phys. Chem. A* **1998**, *102*, 10 300. Chaix, L.; van den Bergh, H.; Rossi, M. J. *J. Phys. Chem. A* **1998**, *103*, 2906.
(26) Abbatt, J. P. D. *Geophys. Res. Lett.* **1994**, *21*, 665.
(27) Hanson, D. R.; Ravishankara, A. R. *Reactions of Halogen Species on Ice Surfaces, in The Tropospheric Chemistry of Ozone in the Polar Regions*; Niki, H., Becker, K. H., Eds., NATO ASI, 1993, *17*, 281.
(28) Allanic, A.; Oppliger, R.; Rossi, M. J. *J. Geophys. Res.* **1997**, *102*, 23 529.
(29) Chu, L.; Chu, L. T. *J. Phys. Chem. A* **1999**, *103*, 8640.
(30) Fenter, F. F.; Caloz, F.; Rossi, M. J. *J. Phys. Chem.* **1994**, *98*, 9801.
(31) Fenter, F. F.; Caloz, F.; Rossi, M. J. *J. Phys. Chem.* **1996**, *100*, 1008.
(32) Dancer, W. *Liebigs Ann. Chem.* **1863**, *125*, 237.
(33) Caloz, F.; Fenter, F. F.; Tabor, K. D.; Rossi, M. J. *Rev. Sci. Instrum.* **1997**, *68*, 3172.
(34) Kumai, M. J. *J. Glaciology* **1968**, *49*, 95.
(35) Westley, M. S.; Baratta, G. A.; Baragiola, R. A. *J. Chem. Phys.* **1998**, *108*, 3321.
(36) Oppliger, R.; Allanic, A.; Rossi, M. J. *J. Phys. Chem.* **1997**, *101*, 1903.
(37) Flückiger, B.; Thielmann, A.; Gutzwiller, L.; Rossi, M. J. *Ber. Bunsen-Ges. Phys. Chem.* **1998**, *102*, 915.
(38) Flückiger, B.; Chaix, L.; Rossi, M. J. *J. Phys. Chem.* **2000** (accepted).
(39) Allanic, A.; Oppliger, R.; Rossi, M. J. submitted to *Phys. Chem. Chem. Phys.* **2000**.
(40) Chu, L. T.; Chu, L. *J. Phys. Chem. A.* **1999**, *103*, 384.
(41) Seisel, S.; Flückiger, B.; Rossi, M. J. *Ber. Bunsen-Ges. Phys. Chem.* **1998**, *102*, 811.
(42) Seisel, S.; Rossi, M. J. *Ber. Bunsen-Ges. Phys. Chem.* **1997**, *101*, 943.